

Macrocyclic Side-Chain Monomers for Photoinduced ATRP: Synthesis and Properties versus Long-Chain Linear Isomers

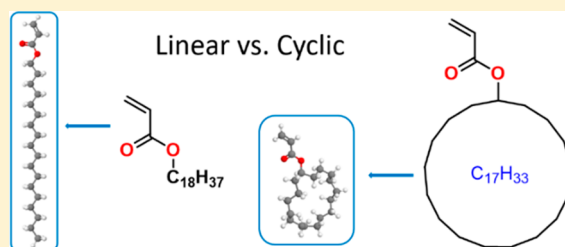
Stephanie M. Barbon,[†] Manon Rolland,[†] Athina Anastasaki,[†] Nghia P. Truong,[§] Morgan W. Schulze,[†] Christopher M. Bates,^{†,‡} and Craig J. Hawker^{*,†,‡}

[†]Materials Research Laboratory and [‡]Materials Department, University of California, Santa Barbara, Santa Barbara, California 93016, United States

[§]ARC Centre of Excellence in Convergent Bio-Nano Science & Technology, Monash Institute of Pharmaceutical Sciences, Monash University, Clayton, VIC 3800, Australia

Supporting Information

ABSTRACT: The photoinduced atom transfer radical polymerization of traditionally challenging hydrophobic monomers (lauryl C₁₂, stearyl C₁₈, and docosyl C₂₂-acrylate) and novel cyclic isomers (C₁₂, C₁₆, and C₁₇) is reported. By the judicious selection of commercially available solvents and catalytic systems, polymers with a high degree of control over dispersity ($\bar{D} \approx 1.1$) and end-group fidelity were obtained over a wide range of molecular weights. This level of control provides access to unique hydrophobic materials (random, block, and homopolymers) with significant differences in properties observed due to the isomeric form of the hydrocarbon side chain (macrocyclic versus linear).



INTRODUCTION

Controlled radical polymerization methods including atom transfer radical polymerization (ATRP),^{1,2} reversible atom transfer fragmentation chain-transfer (RAFT),^{3,4} and nitroxide-mediated polymerization (NMP)^{5,6} have impacted polymer science broadly, allowing for unprecedented control over polymer structure, molecular weight, and end-group fidelity.^{7,8} More recently, visible light has been used as an external stimulus, imparting additional spatial and temporal control over polymer growth by mediating the equilibrium between active and dormant species. Significantly, a variety of different controlled radical polymerization techniques^{9–11} (ATRP,^{12–18} metal-free ATRP,^{19,20} and RAFT^{21–27}) and a range of monomer families,²⁸ such as vinyl ketones, vinyl acetates, and semifluorinated derivatives, have been shown to be amenable to photocontrol.²⁹

In contrast to these advances, the controlled polymerization of long-chain, hydrophobic monomers, such as lauryl (C₁₂), stearyl (octadecyl, C₁₈), and docosyl (behenyl, C₂₂) acrylates, is challenging due to an incompatibility with traditional ATRP catalysts/ligands and, in particular, low-ppm catalytic systems.³⁰ While seemingly simple, only limited examples of controlled radical polymerization of these monomers have been demonstrated, often in expensive solvents, with the majority of these reports focusing on low degrees of polymerization.^{31–35} End-group fidelity at high conversion is also a major issue, restricting diblock copolymer formation to multistep schemes involving purification of macroinitiators, rather than in-situ chain extensions.^{35,36} These challenges conflict with the proven utility of long-chain (C₁₂–C₂₂), hydrophobic monomers for a variety of applications, such as oil

absorbency,³⁷ surfactant swelling,³⁸ low-temperature flow modifiers of oils,³⁹ and particle stabilization.⁴⁰ Block copolymers of these renewable plant-based monomers have also shown interesting self-assembly behavior^{36,41,42} and found use as thermoplastic elastomers⁴³ and polymeric surfactants.⁴⁴ For these applications, one major area of concern is the crystallinity of the linear side chains^{36,45} with many applications requiring high hydrophobicity and amorphous character. To address this challenge, we examined macrocyclic isomers of these long chain linear systems which would be expected to have much lower crystallinity while retaining their very hydrophobic character (Figure 1).⁴⁶ Interestingly, cyclic analogues of long-chain (>6 carbon) hydrocarbon monomers have not been well studied with the only report being the polymerization of cyclododecyl acrylate (C₁₂) under traditional free radical conditions.⁴⁷ Given the importance of this broad class of building blocks, the ability to prepare well-defined materials from long-chain, hydrophobic monomers would significantly enable both fundamental and applied studies.

Herein, the design, synthesis, and characterization of a variety of hydrophobic monomers including linear (C₆–C₂₂) and cyclic (C₆–C₁₇) acrylates, and their polymerization by photoinduced ATRP is described (Figure 2). Low dispersities, good molecular weight control, and excellent chain-end fidelity are obtained leading to facile, in-situ block copolymer synthesis. The resulting copolymers show unique thermal and phase separation behavior, illustrating the potential for

Received: July 16, 2018

Revised: August 14, 2018

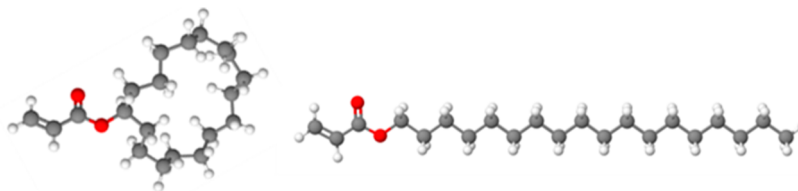


Figure 1. 3D representation of the structural differences between cyclic (C_{17}) and linear (C_{18}) acrylate-based monomers.

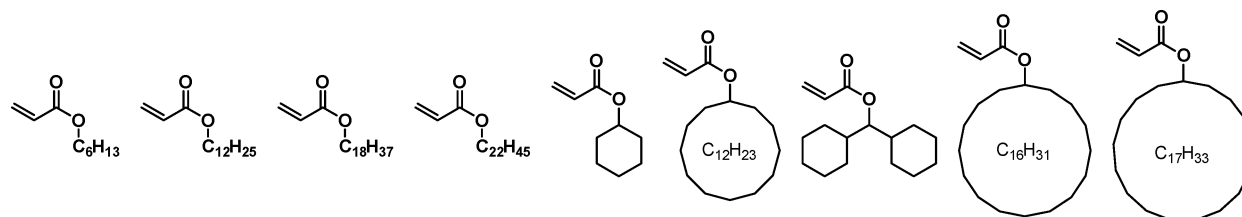


Figure 2. Hydrophobic acrylates used in this study.

using linear versus cyclic side chains to tune physical properties.

EXPERIMENTAL SECTION

All reactions were performed under an argon atmosphere unless otherwise noted and commercially obtained reagents were used as received unless otherwise noted. All reactions were performed in vials, unless otherwise noted. CuBr_2 , 2,2,2-trifluoroethanol, octadecyl acrylate, and hexyl acrylate were purchased from Sigma-Aldrich. Tris[2-(dimethylamino)ethyl]amine (Me_6Tren), acryloyl chloride, cyclododecyl alcohol, and bis(cyclohexyl)methanol were purchased from Alfa Aesar. Lauryl acrylate, cyclohexyl acrylate, behenyl acrylate, and 5-cyclohexadecen-1-one were purchased from TCI Chemicals. Civetone was obtained from Perfumer Supply House.

Nuclear magnetic resonance (NMR) spectra were recorded on a Varian 600 MHz instrument. All ^1H and $^{13}\text{C}\{^1\text{H}\}$ NMR experiments are reported in δ units, parts per million (ppm), and were measured relative to the signal for residual chloroform (7.26 ppm) or deuterated chloroform (77.16 ppm), respectively, in the deuterated solvent unless otherwise stated. Fourier transform infrared (FTIR) spectra were recorded on a PerkinElmer Spectrum 100 FT-IR spectrometer. Size exclusion chromatography (SEC) was performed on a Waters Acquity APC System, with Acquity UPLC PDA and ACQUITY UPLC refractive index detectors. Matrix-assisted laser desorption/ionization time-of-flight mass spectrometry (MALDI-ToF-MS) was conducted using a Bruker Microflex LRF MALDI TOF mass spectrometer equipped with a 60 Hz nitrogen laser at 337 nm. Solutions in tetrahydrofuran of dithranol as a matrix (saturated solution, 10 μL) and sodium bromide as cationization agent (1.0 mg/mL, 2 μL) were mixed with the sample (1.0 mg/mL, 10 μL), and 0.7 μL of the mixture was applied to the target plate. Differential scanning calorimetry (DSC) measurements were performed using a Q2000 DSC V24.11 instrument from -160 to 100 $^\circ\text{C}$ at a heating and cooling rate of 10 $^\circ\text{C}/\text{min}$ (N_2 flow of 50 mL/min). The polymerization light source (UV: $\lambda_{\text{max}} \approx 360$ nm) was a commercial nail curing lamp (Thermal Spa, obtained online from Amazon) equipped with 3×16 W bulbs.

Reduction of Civetone to Cycloheptadecanol. Palladium on carbon (0.20 g, 0.10 mmol Pd) was added to a dry 100 mL round-bottom flask. Isopropanol (50 mL) was added, followed by civetone (5.00 g, 20 mmol) and acetic acid (2.40 g, 40 mmol, 2.28 mL). With stirring, sodium borohydride (4.53 g, 120 mmol) was added, and rapid bubbling occurred. The reaction mixture was stirred for 14 h open to the atmosphere. Excess NaBH_4 was quenched with 0.1 M HCl, with addition continuing until no further gas evolved. The pH was then increased to 10 with 1 M KOH; the solution was filtered through Celite and transferred to a separatory funnel. The reaction mixture was extracted three times with dichloromethane (100 mL).

The organic fractions were combined, dried over MgSO_4 , gravity filtered, and concentrated *in vacuo* to give cycloheptadecanol. Yield = 4.86 g (95%). ^1H NMR (599.8 MHz, CDCl_3): δ 3.70 (p, $J = 6$ Hz, 1H, HO-CH), 1.31–1.55 (m, 32H, alkyl CH_2). ^{13}C NMR (100.6 MHz, CDCl_3): δ 71.0, 35.9, 28.0, 27.8, 27.7, 27.6, 27.6, 27.5, 23.9. FT-IR (ATR cm^{-1}): 3309, 2921, 2853, 1458, 1351, 1291, 1086, 1012, 715. HRMS (GC-MS) exact mass calcd for $\text{C}_{17}\text{H}_{34}\text{O}$ [$\text{M}-\text{H}_2\text{O}$] $^+$: 236.2504; found: 236.2499.

Reduction of 5-Cyclohexadecen-1-one to Cyclohexadecanol. Palladium on carbon (0.42 g, 0.42 mmol Pd) was added to a dry 500 mL round-bottom flask. Isopropanol (200 mL) was added, followed by 5-cyclohexadecen-1-one (10.00 g, 42.3 mmol) and acetic acid (5.08 g, 84.6 mmol, 4.84 mL). With stirring, sodium borohydride (9.60 g, 254 mmol) was added, and rapid bubbling occurred. The reaction mixture was stirred for 14 h open to the atmosphere. Excess NaBH_4 was quenched with 0.1 M HCl, with addition continuing until no further gas evolved. The pH was then increased to 10 with 1 M KOH; the solution was filtered through Celite and transferred to a separatory funnel. The reaction mixture was extracted three times with dichloromethane (100 mL). The organic fractions were combined, dried over MgSO_4 , gravity filtered, and concentrated *in vacuo* to give cyclohexadecanol. Yield = 9.56 g (94%). ^1H NMR (599.8 MHz, CDCl_3): δ 3.73 (p, $J = 6$ Hz, 1H, HO-CH), 1.53–1.57 (m, 2H, alkyl CH_2), 1.44–1.48 (m, 2H, alkyl CH_2), 1.31–1.37 (m, 26H, alkyl CH_2). ^{13}C NMR (100.6 MHz, CDCl_3): δ 70.7, 35.2, 27.2, 27.0, 26.8, 26.8, 26.7, 23.4. FT-IR (ATR cm^{-1}): 3301, 2923, 2853, 1459, 1348, 1299, 1026, 996, 709. HRMS (GC-MS) exact mass calcd for $\text{C}_{16}\text{H}_{32}\text{O}$ [$\text{M}-\text{H}_2\text{O}$] $^+$: 222.2348; found: 222.2346.

General Procedure for the Preparation of Monomers. Under argon, the appropriate alcohol (0.016 mol) was dissolved in dry dichloromethane (50 mL) containing triethylamine (2.43 g, 3.34 mL, 0.024 mol) in a 100 mL Schlenk flask. This solution was cooled for 25 min in an ice bath. Acryloyl chloride (2.21 g, 1.94 mL, 0.024 mol) was then added slowly to the cooled alcohol solution, which gradually turns a light yellow color. The mixture was stirred in an ice bath for an additional 4 h. The solution was transferred to a separatory funnel, washed with 1 M KOH (100 mL), 1 M HCl (100 mL), and brine solution (100 mL), dried over MgSO_4 , gravity filtered, and concentrated *in vacuo*. The resulting residue was purified by column chromatography (1:1 CH_2Cl_2 :hexanes, silica) to yield the monomer as a colorless liquid.

Cyclododecyl Acrylate. Prepared from 2.95 g (16.0 mmol) of cyclododecanol. Yield = 2.78 g (73%). ^1H NMR (599.8 MHz, CDCl_3): δ 6.37 (d, $J = 17$ Hz, 1H, vinyl CH), 6.10 (dd, $J = 17, 10$ Hz, 1H, vinyl CH) 5.78 (d, $J = 10$ Hz, 1H, vinyl CH), 5.07–5.11 (m, 1H, tertiary CH), 1.71–1.77 (m, 2H, alkyl CH_2), 1.52–1.57 (m, 2H, alkyl CH_2), 1.32–1.45 (m, 18H, alkyl CH_2). ^{13}C NMR (100.6 MHz, CDCl_3): δ 166.1, 130.1, 129.3, 72.6, 29.2, 24.3, 24.0, 23.5, 23.4, 21.0.

FT-IR (ATR cm^{-1}): 2934, 2921, 2850, 1721, 1404, 1296, 1273, 1197, 1047, 984, 960. HRMS (ESI) exact mass calcd for $\text{C}_{15}\text{H}_{26}\text{O}_2$ [$\text{M}-\text{Na}$] $^+$: 261.1830; found: 261.1830.

Bis(cyclohexyl) Acrylate. Prepared from 3.15 g (16.0 mmol) of dicyclohexylmethanol. Yield = 2.73 g (68%). ^1H NMR (599.8 MHz, CDCl_3): δ 6.40 (d, $J = 17$ Hz, 1H, vinyl CH), 6.13 (dd, $J = 17, 10$ Hz, 1H, vinyl CH) 5.81 (d, $J = 10$ Hz, 1H, vinyl CH), 4.71 (t, $J = 6$ Hz, 1H, tertiary CH), 1.60–1.74 (m, 12H, alkyl CH_2), 0.87–1.26 (m, 10H, alkyl CH_2). ^{13}C NMR (100.6 MHz, CDCl_3): δ 166.5, 130.3, 129.0, 81.7, 38.6, 30.0, 27.6, 26.5, 26.4, 26.2. FT-IR (ATR cm^{-1}): 2921, 2915, 2852, 1723, 1443, 1402, 1295, 1269, 1188, 1042, 984, 966. HRMS (ESI) exact mass calcd for $\text{C}_{16}\text{H}_{26}\text{O}_2$ [$\text{M}-\text{Na}$] $^+$: 273.1830; found: 273.1820.

Cyclohexadecyl Acrylate. Prepared from 10.17 g (42.3 mmol) of cyclohexadecanol. Yield = 7.97 g (64%). ^1H NMR (599.8 MHz, CDCl_3): δ 6.37 (dd, $J = 17.3, 1.5$ Hz, 1H, vinyl CH), 6.10 (dd, $J = 17.3, 10.4$ Hz, 1H, vinyl CH) 5.78 (dd, $J = 10.4, 1.5$ Hz, 1H, vinyl CH), 4.99 (p, $J = 6.1$ Hz, 1H, tertiary CH), 1.58–1.67 (m, 4H, alkyl CH_2), 1.32–1.39 (m, 26H, alkyl CH_2). ^{13}C NMR (100.6 MHz, CDCl_3): δ 166.1, 130.2, 129.3, 74.0, 31.9, 27.1, 27.0, 26.8, 26.8, 26.8, 26.7, 23.3. FT-IR (ATR cm^{-1}): 2925, 2857, 1721, 1619, 1461, 1404, 1293, 1271, 1194, 1045, 984, 962, 809. HRMS (GC-MS) exact mass calcd for $\text{C}_{19}\text{H}_{34}\text{O}_2$ [$\text{M}-\text{C}_2\text{H}_4\text{O}_2$] $^+$: 222.2348; found: 222.2358.

Cycloheptadecyl Acrylate. Prepared from 1.60 g (63.4 mmol) of cycloheptadecanol. Yield = 1.38 g (71%). ^1H NMR (599.8 MHz, CDCl_3): δ 6.38 (d, $J = 17$ Hz, 1H, vinyl CH), 6.10 (dd, $J = 17, 11$ Hz, 1H, vinyl CH) 5.79 (d, $J = 11$ Hz, 1H, vinyl CH), 4.93–4.97 (m, 1H, tertiary CH), 1.58–1.66 (m, 4H, alkyl CH_2), 1.32–1.37 (m, 28H, alkyl CH_2). ^{13}C NMR (100.6 MHz, CDCl_3): δ 166.1, 130.2, 129.3, 74.2, 32.5, 27.9, 27.8, 27.7, 27.6, 27.5, 27.4, 23.8. FT-IR (ATR cm^{-1}): 2924, 2856, 1722, 1621, 1461, 1404, 1295, 1272, 1196, 1046, 985, 810. HRMS (ESI) exact mass calcd for $\text{C}_{20}\text{H}_{36}\text{O}_3$ [$\text{M}-\text{Na}$] $^+$: 331.2613; found: 331.2628.

General Polymerization Procedure. A stock solution of copper(II) bromide (2.2 mg, 0.0098 mmol) and Me_6Tren (13.9 mg, 16.1 μL , 0.060 mmol) was prepared in 1 mL of trifluoroethanol. In a 20 mL scintillation vial, hexyl acrylate (0.50 g, 3.21 mmol) was dissolved in a mixture of 0.4 mL of toluene and 0.1 mL of the Cu(II)/trifluoroethanol stock solution. Ethyl α -bromoisobutyrate (EBiB, 9.8 mg, 0.05 mmol) was then added, the vial was capped with a septum, and the solution was degassed with argon for 5 min. With stirring, the polymerization mixture was then irradiated ($\lambda \approx 360$ nm) for 8 h in a commercial UV nail lamp system. The resulting polymer was purified via dissolution in a minimal amount of toluene and precipitation in cold methanol three times.

Poly(*n*-hexyl acrylate). Synthesized from 0.5 g (3.2 mmol) of *n*-hexyl acrylate and 9.8 mg (0.050 mmol) of EBiB in 0.5 mL of the solvent mixture. Yield = 0.36 g (72%). ^1H NMR (599.8 MHz, CDCl_3): δ 4.01 (2H), 1.88–2.35 (2H), 1.45–1.61 (3H), 1.31 (6H), 0.90 (3H). SEC: $M_n = 6400$ g/mol, $\bar{D} = 1.08$.

Poly(cyclohexyl acrylate). Synthesized from 1.0 g (6.5 mmol) of cyclohexyl acrylate and 19.6 mg (0.10 mmol) of EBiB in 1.0 mL of the solvent mixture. Yield = 0.81 g (81%). ^1H NMR (599.8 MHz, CDCl_3): δ 4.69 (1H), 2.24–2.31 (1H), 1.23–1.82 (12H), 1.11 (d, 0.15 H). SEC: $M_n = 7400$ g/mol, $\bar{D} = 1.07$.

Poly(lauryl acrylate). Synthesized from 2.0 g (8.3 mmol) of lauryl acrylate and 39.0 mg (0.20 mmol) of EBiB in 2.0 mL of the solvent mixture. Yield = 1.68 g (84%). ^1H NMR (599.8 MHz, CDCl_3): δ 4.01 (2H), 2.19–2.32 (2H), 1.01–1.91 (21H), 0.88 (t, 3H). SEC: $M_n = 6600$ g/mol, $\bar{D} = 1.05$.

Poly(cyclododecyl acrylate). Synthesized from 0.3 g (1.3 mmol) of cyclododecyl acrylate and 5.6 mg (0.029 mmol) of EBiB in 0.3 mL of the solvent mixture. Yield = 0.23 g (77%). ^1H NMR (599.8 MHz, CDCl_3): δ 4.95 (1H), 2.25 (1H), 1.36–1.84 (24H). ^{13}C NMR (150.8 MHz, CDCl_3): δ 174.1, 72.6, 41.5, 29.2, 24.5, 23.5, 21.1. SEC: $M_n = 4600$ g/mol, $\bar{D} = 1.14$. FT-IR (ATR cm^{-1}): 2921, 2852, 1725, 1447, 1250, 1161, 1094, 907.

Poly(bis(cyclohexyl) acrylate). Synthesized from 0.7 g (2.8 mmol) of bis(cyclohexyl) acrylate and 13.6 mg (0.070 mmol) of EBiB in 0.7 mL of the solvent mixture. Yield = 0.60 g (85%). ^1H NMR

(599.8 MHz, CDCl_3): δ 4.63 (1H), 2.59 (1H), 1.01–2.07 (24H). ^{13}C NMR (150.8 MHz, CDCl_3): δ 174.4, 81.2, 41.6, 38.7, 30.1, 27.9, 26.6. SEC: $M_n = 2600$ g/mol, $\bar{D} = 1.11$. FT-IR (ATR cm^{-1}): 2921, 2851, 1725, 1448, 1248, 1160, 1092, 965, 907.

Poly(cyclohexadecyl acrylate). Synthesized from 0.5 g (1.7 mmol) of cyclohexadecyl acrylate and 3.9 mg (0.020 mmol) of EBiB in 0.5 mL of the solvent mixture. Yield = 0.42 g (84%). ^1H NMR (599.8 MHz, CDCl_3): δ 4.82 (1H), 2.23–2.29 (1H), 1.55–1.89 (7H), 1.32 (27H). ^{13}C NMR (150.8 MHz, CDCl_3): δ 174.0, 73.9, 41.9, 41.4, 31.8, 27.2, 26.8, 26.7, 26.7, 23.5, 23.4. SEC: $M_n = 5800$ g/mol, $\bar{D} = 1.21$. FT-IR (ATR cm^{-1}): 2924, 2856, 1728, 1461, 1348, 1256, 1161, 1034.

Poly(cycloheptadecyl acrylate). Synthesized from 0.5 g (1.6 mmol) cycloheptadecyl acrylate, and 9.8 mg (0.050 mmol) EBiB in 0.5 mL of the solvent mixture. Yield = 0.39 g (78%). ^1H NMR (599.8 MHz, CDCl_3): δ 4.78 (1H), 1.80–2.21 (1H), 1.11–1.60 (34H). ^{13}C NMR (150.8 MHz, CDCl_3): δ 173.8, 74.2, 41.9, 41.4, 32.5, 28.0, 27.7, 27.6, 27.3, 23.9. SEC: $M_n = 3400$ g/mol, $\bar{D} = 1.14$. FT-IR (ATR cm^{-1}): 2922, 2855, 1728, 1459, 1348, 1253, 1160, 1033, 728.

Poly(*n*-octadecyl acrylate). Synthesized from 0.5 g (1.5 mmol) of *n*-octadecyl acrylate and 9.7 mg (0.050 mmol) of EBiB in 0.5 mL of the solvent mixture. Yield = 0.35 g (71%). ^1H NMR (599.8 MHz, CDCl_3): δ 4.01 (2H), 2.27–2.34 (1H), 1.89–2.02 (1H), 1.60 (3H), 1.26–1.30 (30 H), 0.88 (t, 3H). SEC: $M_n = 3500$ g/mol, $\bar{D} = 1.12$.

Poly(docosyl acrylate). Synthesized from 1.0 g (2.6 mmol) of docosyl acrylate and 7.8 mg (0.040 mmol) of EBiB in 1.1 mL of the solvent mixture. Yield = 0.79 g (79%). ^1H NMR (599.8 MHz, CDCl_3): δ 4.00 (2H), 1.59 (3H), 1.25–1.30 (40 H), 0.88 (t, $J = 7$ Hz, 3H). SEC: $M_n = 9800$ g/mol, $\bar{D} = 1.13$.

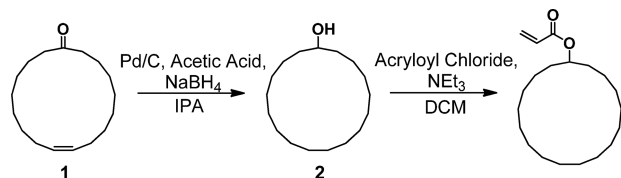
General Procedure for Diblock Copolymer Formation. A stock solution of copper(II) bromide (4.2 mg, 0.019 mmol) and Me_6Tren (25.6 mg, 29.7 μL , 0.11 mmol) was prepared in 0.4 mL of trifluoroethanol. In a 20 mL scintillation vial, cyclododecyl acrylate (0.50 g, 2.09 mmol) was dissolved in a mixture of 0.4 mL of toluene and 0.1 mL of the trifluoroethanol stock solution. EBiB (4.5 mg, 0.02 mmol) was then added, the vial was capped with a septum, and the solution was degassed with argon for 5 min. With stirring, the polymerization mixture was then irradiated with ≈ 360 nm light for 8 h in a commercial UV nail lamp system. A second vial, charged with 0.1 mL of the trifluoroethanol stock solution, 0.3 mL of trifluoroethanol, 1.6 mL of toluene, and *tert*-butyl acrylate (2.32 g, 18.1 mmol), was then degassed with argon for 5 min, and the contents were transferred by syringe to the polymerization vial. This mixture was returned to the UV nail lamp and irradiated with ≈ 360 nm light with stirring for an additional 8 h. The resulting polymer was purified via dissolution in a minimal amount of toluene and precipitation in cold methanol three times.

RESULTS AND DISCUSSION

To increase the range of well-defined hydrophobic polymers, two structural libraries of monomers with side chains of varied carbon number configured in a linear or macrocyclic form were examined under photoinduced ATRP conditions. Hexyl acrylate (L-6), lauryl acrylate (L-12), octadecyl acrylate (L-18), and docosyl acrylate (L-22) with 6, 12, 18, and 22 carbons in the side chain, respectively, were chosen as linear monomers, while cyclohexyl acrylate (C-6), cyclododecyl acrylate (C-12), bis(cyclohexyl acrylate) (C-13), cyclohexadecyl acrylate (C-16), and cycloheptadecyl acrylate (C-17) with 6–17 carbons in the side chain were selected as macrocyclic analogues. To illustrate the synthetic utility inherent in these novel macrocyclic side chains, readily available macrocyclic ketones were selected as starting materials, and highly efficient chemistry was developed to convert these systems to the desired acrylate derivatives. For example, C-17 was designed starting from civetone, a commercially available fragrance additive. As shown in Scheme

1, room temperature reduction and hydrogenation of civetone, 1, was achieved in a one-pot process to give the desired

Scheme 1. Synthesis of Cycloheptadecyl Acrylate, C-17, Monomer from Civetone, 1

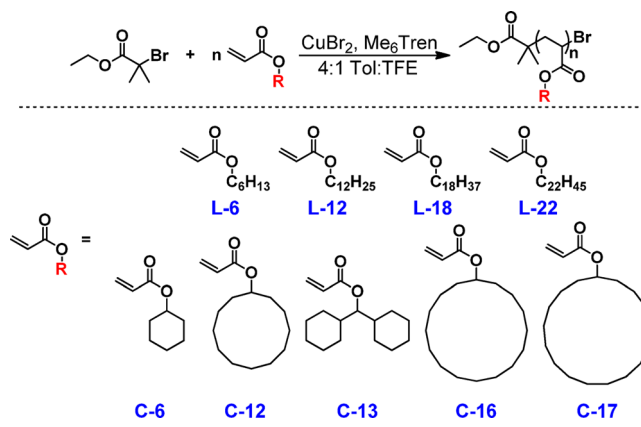


cycloheptadecyl alcohol, 2. As with the other commercially available cyclic alcohols, such as cyclododecyl alcohol which is a precursor for nylon-6-12, esterification with acryloyl chloride leads to the acrylate derivative in excellent yields (Scheme 1 and Figures S1–S10). This synthetic pathway is amenable to other similar starting materials with C-16 being synthesized in the same manner. These macrocyclic isomers of traditional long-chain acrylate monomers have similar hydrophobicity but are expected to have significantly different crystallization properties due to the inability of the side chains to interdigitate.

As a simple and versatile polymerization protocol, our efforts were directed to photoinduced ATRP^{14,17} with the initial challenge being to identify polymerization conditions that allow for a wide range of molecular weights to be synthesized with good control and high end-group fidelity. A critical feature is selection of a solvent system which solubilizes both the very hydrophobic monomers and resulting polymers as well as the hydrophilic copper/ligand catalyst (Cu(II)/Me₆Tren). Traditional solvents like DMSO were not effective and in accordance with previous studies led to poor molecular weight control with dispersities of >2.0.³⁰ Toluene was shown to have increased utility with the monomers and resulting polymers soluble; however, the copper/ligand catalyst was sparingly soluble, leading to only a moderate decrease in dispersity. To address these opposing solubility requirements, a range of cosolvents with toluene such as isopropanol, methanol, and DMSO were therefore investigated, with little or no control being observed. In direct contrast, trifluoroethanol (TFE)^{48–50} showed promise as a cosolvent, with a 4:1 ratio of toluene:TFE solubilizing all components of the reaction mixture. Significantly, good control and high reproducibility for the polymerization of all hydrophobic monomers were achieved with a CuBr₂ and Me₆Tren catalytic system using ethyl α -bromoisobutyrate (EBiB) as the initiator (Scheme 2).

The controlled photopolymerization of hydrophobic monomers was initially studied with the library of linear, long-chain C₆, C₁₂, C₁₈, and C₂₂ derivatives: L-6, L-12, L-18, and L-22. Significantly, polymerization kinetics for lauryl acrylate at a low theoretical DP of 20 showed a linear increase of $\ln[M]_0/[M]_t$ with time, confirming the controlled nature of the process in 4:1 toluene/TFE (see Figure S13). Building from this observation, a major requirement for these systems is to maintain solubility of the growing polymer chains with increasing molecular weight. It was therefore important to show that polymers with a wide range of molar masses could be synthesized with a high degree of control. To illustrate this, a series of poly(lauryl acrylate) polymers were synthesized, ranging in theoretical molar masses from 2000 to 100000 g/mol. For low molecular weight polymers, good agreement is

Scheme 2. Polymerization Scheme for Hydrophobic Linear and Cyclic Monomers, Including Hexyl (L-6), Lauryl (L-12), Octadecyl (L-18), Docosyl (L-22), Cyclohexyl (C-6), Cyclododecyl (C-12), Bis(cyclohexyl) (C-13), Cyclohexadecyl (C-16), and Cycloheptadecyl Acrylate (C-17)



observed between the targeted and observed degree of polymerization by ¹H NMR spectroscopy (see Table 1). At higher molecular weights, end-group analysis by NMR spectroscopy is not reliable; however, SEC clearly indicates well-defined increases in molecular weight, and symmetrical, low-dispersity peaks are evident (see Figure 3). The disparity between molecular weight measured by SEC and targeted molecular weight is attributed to the inherent hydrodynamic differences of the linear polystyrene calibrants and our polymer samples. In each case, good molecular weight control was maintained, with all dispersities ≤ 1.11 (see Figure 3 and Table 1, entries 3–8). This is in contrast to other reported conditions for the polymerization of lauryl acrylate, where degrees of polymerization over 50 ($M_n \approx 12000$) could not be targeted, and at lower DPs, increased dispersity was observed.⁵¹

Extension of these conditions to other linear side-chain monomers proved successful with homopolymers of all monomers reaching >98% conversion within 8 h, with low dispersities (see Table 1 and Figures S14–S19). Matrix-assisted laser-desorption ionization (MALDI) was utilized to examine the end-group fidelity for these different hydrophobic polymers. With all linear side-chain systems, high end-group fidelity was maintained, with the bromine chain end clearly observed in molecular ion peaks, suggesting minimal termination or side reactions. Additionally, the m/z for each system confirmed the presence of the ethyl isobutyrate initiating group on the α -chain end (see Figures S20–S22).

This high degree of end-group fidelity and compatibility with different side-chain lengths prompted an examination of chain extension and formation of in-situ block copolymers (Table S1). *tert*-Butyl acrylate was selected as a functional comonomer, which after deprotection would lead to novel diblock copolymers composed of disparate hydrophobic and hydrophilic blocks. From an initial short block of poly(lauryl acrylate) (DP 9, M_n (NMR) = 2400 g/mol, 99% conversion), *tert*-butyl acrylate was added directly into the reaction mixture with additional catalyst and solvent; the resulting polymer obtained an overall molar mass of ≈ 12000 g/mol (NMR) and a degree of polymerization for the *tert*-butyl acrylate block of ≈ 80 , in agreement with expected block lengths. The SEC trace (Figure 4, top) shows efficient chain extension, with the final

Table 1. Homopolymers of Hydrophobic Monomers Synthesized by Photoinduced ATRP (All Polymers Reached Conversions of >98%)

polymer	$M_n(\text{SEC})^{b,c}$	$M_n(\text{NMR})^{a,c}$	DP(NMR) ^a	DP(theor)	$M_n^c(\text{theor})$	$\mathcal{D}(\text{SEC})^b$
poly(L-6)	1600	2200	13	13	2200	1.14
	6400			64	10200	1.08
poly(L-12)	2000	2200	8	9	2400	1.11
	4000			21	5200	1.07
	6600			42	10300	1.05
	12600			104	25200	1.07
	29400			250	60300	1.08
	50700			417	100400	1.07
poly(L-18)	2300	2000	6	6	2100	1.09
	4900			31	10300	1.08
	11400			77	25200	1.09
poly(L-22)	9800			66	25300	1.13

^aDue to the overlap between initiator signals from the initiator and the side-chain in the ¹H NMR spectrum, these values could only be calculated reliably for low molar mass polymers. ^bRelative to polystyrene standards. ^cIn units of g/mol.

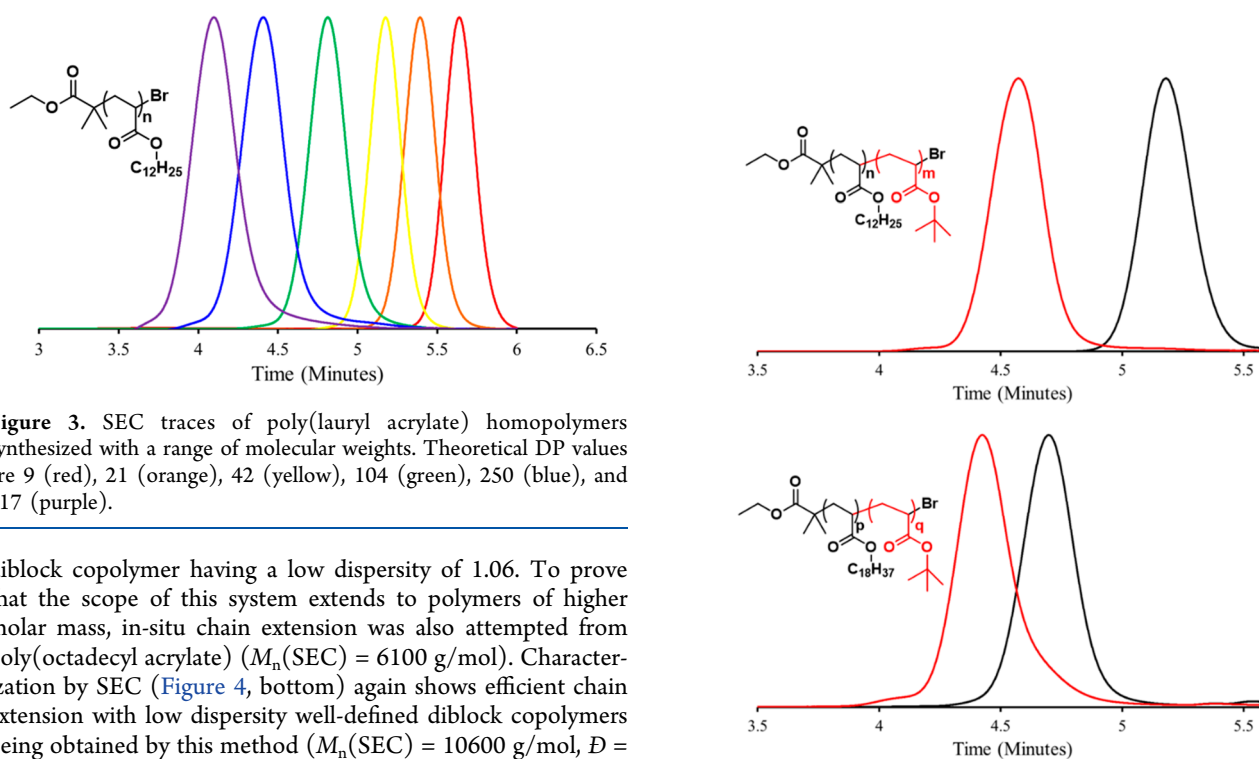


Figure 3. SEC traces of poly(lauryl acrylate) homopolymers synthesized with a range of molecular weights. Theoretical DP values are 9 (red), 21 (orange), 42 (yellow), 104 (green), 250 (blue), and 417 (purple).

diblock copolymer having a low dispersity of 1.06. To prove that the scope of this system extends to polymers of higher molar mass, in-situ chain extension was also attempted from poly(octadecyl acrylate) ($M_n(\text{SEC}) = 6100$ g/mol). Characterization by SEC (Figure 4, bottom) again shows efficient chain extension with low dispersity well-defined diblock copolymers being obtained by this method ($M_n(\text{SEC}) = 10600$ g/mol, $\mathcal{D} = 1.13$). These examples clearly illustrate the potential of photoinduced ATRP under these optimized polymerization conditions for in-situ block copolymerization using very hydrophobic building blocks.

With the advances described above for long-chain linear hydrophobic monomers, our attention was then directed to macrocyclic isomers. It is noteworthy that this monomer class is surprisingly understudied, despite the potential for markedly different properties when compared to their linear analogues.⁴⁶ In this work, the polymerization of a broad spectrum of cyclic monomers C-6, C-12, C-13, C-16, and C-17 was examined. Initial observations proved to warrant study with the polymerization of bis(cyclohexyl) acrylate proceeding much slower than linear analogues, often requiring 18 h to reach full conversion, though good dispersities were still achieved, likely due to the steric bulk of the monomer ($\mathcal{D} \leq 1.11$, Table 2 and Figures S23, S24). In contrast, the rates of polymerization of cycloheptadecyl acrylate, cyclohexadecyl acrylate, cyclododecyl acrylate, and cyclohexyl acrylate are similar to that of lauryl

Figure 4. Diblock copolymers of poly(lauryl acrylate-*block-tert*-butyl acrylate), $n \approx 8$, $m \approx 80$ (top) and poly(octadecyl acrylate-*block-tert*-butyl acrylate), $p \approx 30$, $q \approx 80$ (bottom).

acrylate, with full conversion reached within 8 h and with good dispersities (Table 2 and Figures S25–S30) and a linear increase of $\ln[M]_0/[M]_t$ with time (Figure S31), using the conditions described above (Figures S32–S39). As an illustrative example, cyclododecyl acrylate shows a linear evolution of molar mass with conversion. Aliquots were taken from the reaction mixture every hour, and SEC analysis of the crude reaction mixture shows a linear dependence of M_n on conversion, with consistently low dispersity ($\mathcal{D} \approx 1.10$, Figure 5).

In addition, SEC characterization displayed narrow peaks over a wide range of molar masses (from 2000 to 100000 g/mol, see Figure 6) with good correlation between experimental

Table 2. Homopolymers of Hydrophobic Monomers Synthesized by Photoinduced ATRP (All Polymers Reached Conversions of >98%)

polymer	$M_n(\text{SEC})^b$	$M_n(\text{NMR})^a$	DP(NMR) ^a	DP(theor)	$M_n^c(\text{theor})$	$D(\text{SEC})^b$
poly(C-6)	1500	2000	12	13	2200	1.13
	7400			65	10200	1.07
poly(C-12)	1200	2200	8	8	2100	1.13
	2600	4400	18	21	5200	1.14
	4600			42	10200	1.14
	8000			105	25200	1.09
	18100			252	60300	1.09
	29500			420	100300	1.10
poly(C-13)	850			8	2200	1.09
	2600			40	10200	1.11
poly(C-16)	5800			85	25200	1.18
poly(C-17)	930	2100	7	6	2100	1.13
	3400			32	10100	1.14
	8000			81	25300	1.15

^aDue to the overlap between initiator signals from the initiator and the side chain in the ¹H NMR spectrum, these values could only reliably be calculated for low molar mass polymers. ^bRelative to polystyrene standards. ^cIn units of g/mol.

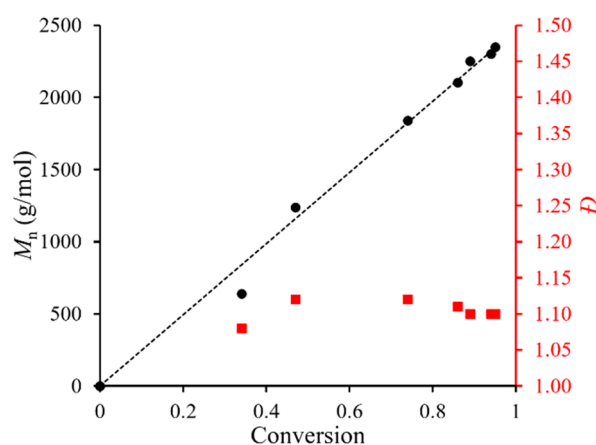


Figure 5. Kinetic data for the homopolymerization of cyclododecyl acrylate, C-12, showing a linear evolution of molar mass with conversion and low dispersities.

(¹H NMR analysis) and theoretical values for low DP samples (Table 2, entries 3 and 4).

Further structural confirmation was obtained from MALDI-TOF analysis which showed one major set of molecular ions

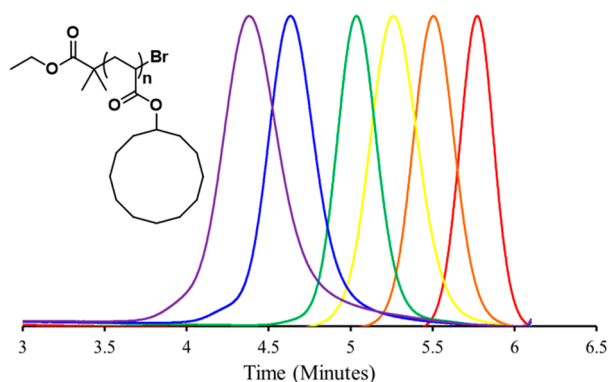


Figure 6. SEC traces of poly(cyclododecyl acrylate) homopolymers synthesized over a range of molecular weights. Theoretical n values are 8 (red), 21 (orange), 42 (yellow), 105 (green), 252 (blue), and 420 (purple).

for all cyclic side-chain monomers corresponding to the expected bromine end group and ethyl isobutyrate initiating group (Figure 7, Figures S40 and S41). It should be noted that for all samples, including linear side chains, MALDI spectra collected at higher laser power (55%) revealed a small second set of peaks corresponding to chain–chain coupling. These peaks increased in intensity with increased laser power (see Figure S42) and were observed in similar proportion at low and high conversions, further reinforcing their artifact nature (see Figure S43).

To initially monitor block copolymer formation, a short block of cycloheptadecyl acrylate (DP(NMR) 6, $M_n(\text{NMR}) \approx 2000$ g/mol) was polymerized to >98% conversion and then chain extended in situ with *tert*-butyl acrylate. The resulting polymer had a dispersity of 1.18 by SEC and an overall $M_n(\text{NMR})$ of 12600 g/mol, illustrating high fidelity for chain extension and the ability to prepare block copolymers with significantly different block sizes (DP = 6 and 82) (Figure 8, top). In-situ chain extension to give blocks of comparable molecular weight was then demonstrated from an initial cyclododecyl acrylate block (DP \approx 42) with chain extension proceeding as expected (*tert*-butyl acrylate, DP \approx 80), resulting in a diblock copolymer with low dispersity and controlled molecular weight (Figure 8, bottom). As shown in Figures S44–S46, other block ratios and monomer units can be used to prepare a wide range of hydrophobic block copolymers using in-situ procedures.

A major driver for these very hydrophobic systems is the thermal properties of the macrocyclic isomers and comparison with the long chain, linear materials. Initially, the homopolymers of each monomer with a common molecular weight of ≈ 10000 g/mol were examined. As expected, a significant difference in thermal properties between the linear, long-chain derivatives and their macrocyclic analogues is evident. This is exemplified in the differential scanning calorimetry thermograms for polymers based on side chains containing 12 or 13 carbon atoms (L-12, C-12, and C-13, see Figures S47–S49). Poly(lauryl acrylate), with a linear 12-carbon side chain, exhibits a melt transition (T_m) at -5.0 °C due to the interdigitation of the side chains. In contrast, poly(cyclododecyl acrylate) shows only a glass transition temperature, T_g of -20 °C, with no observable melting transition

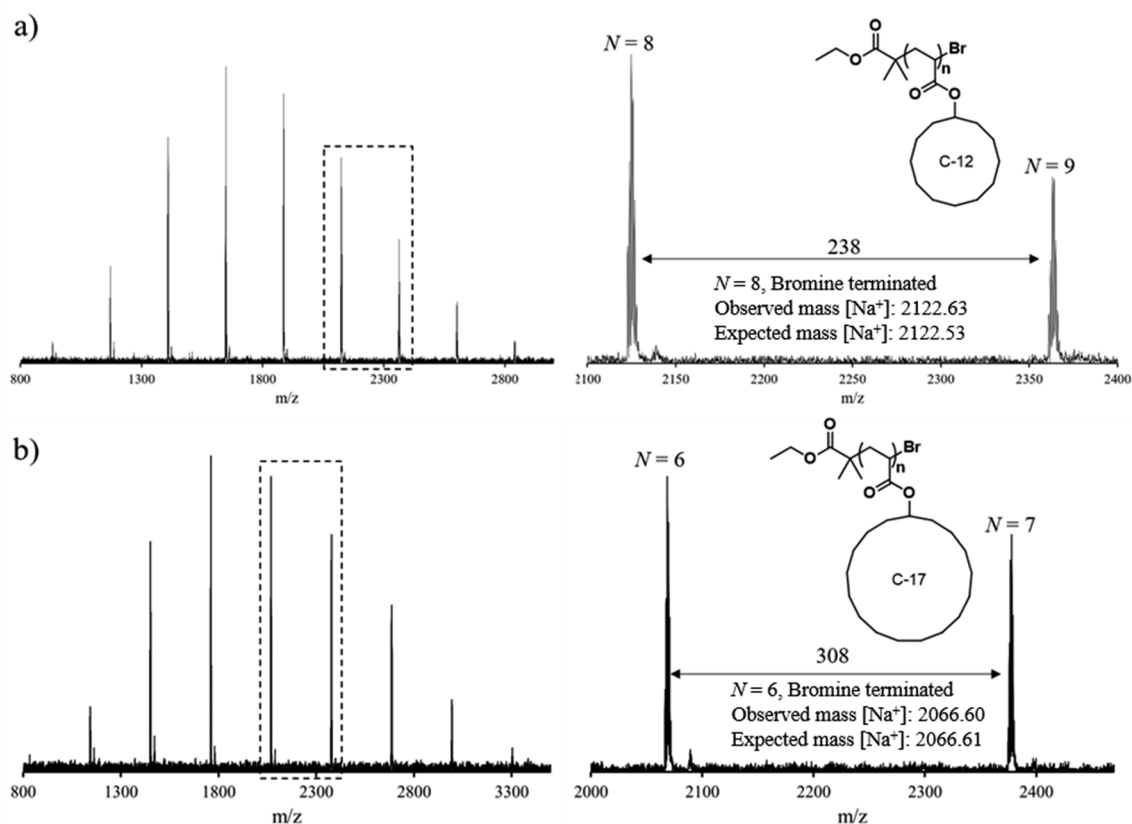


Figure 7. MALDI-ToF-MS analysis for (a) poly(C-12) and (b) poly(C-17). Magnified regions show the expected monomer spacing and Br termination.

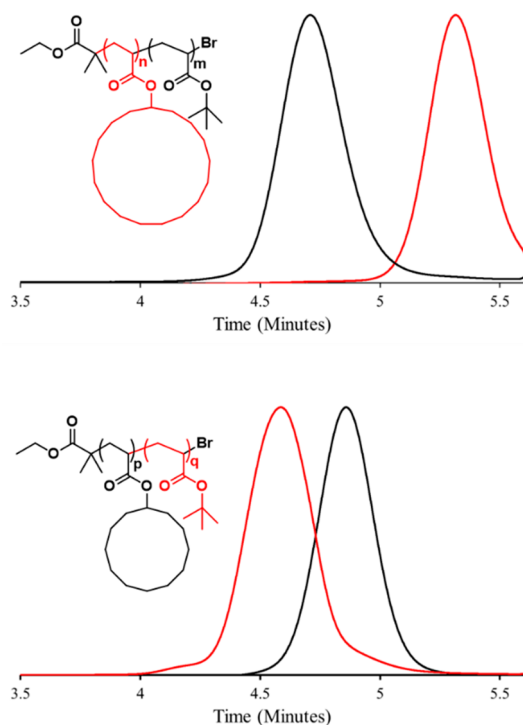


Figure 8. DSC analysis of diblock copolymers of poly(cycloheptadecyl acrylate-*block-tert*-butyl acrylate), $n \approx 6$, $m \approx 78$ (top) and poly(cyclododecyl acrylate-*block-tert*-butyl acrylate), $p \approx 42$, $q \approx 78$ (bottom).

while poly(bis(cyclohexyl) acrylate) exhibited a significantly increased glass transition of 28 °C. This difference in thermal behavior is even more pronounced for longer alkyl side chains with the linear 18-membered side chain of poly(octadecyl acrylate), resulting in an increase in the melting transition to 47 °C and the 17-membered macrocyclic side chain of poly(cycloheptadecyl acrylate) showing a significantly lower glass transition of -25 °C. The variation in crystallization behavior and glass transition temperature is fully in agreement with tendency of the linear side chains to interdigitate and the cyclic side chains to pack inefficiently. All thermal transitions of known polymers are consistent with literature values (see Table 3).^{52,53}

This important difference between long-chain, linear and macrocyclic acrylate monomers with the same or similar number of carbon atoms was further illustrated by examining

Table 3. Thermal Properties of Polymers

polymer	no. of C's in monomer side chain	T_m (lit.) (°C)	T_g (lit.) (°C)
poly(L-6)	6		-66 (-57) ⁵³
poly(C-6)	6		9 (19) ⁵³
poly(L-12)	12	-5 (-3) ⁵³	
poly(C-12)	12		-20
poly(C-13)	13		28
poly(C-16)	16		-19
poly(C-17)	17		-25
poly(L-18)	18	47 (41) ⁵²	
poly(L-22)	22	65 (71) ⁵⁴	

the diblock copolymer consisting of a $\sim 1:1$ molar ratio of octadecyl acrylate (L-18) and cycloheptadecyl acrylate (C-17). This copolymer was synthesized according to the procedure described above, with in-situ growth of the octadecyl acrylate block from poly(cycloheptadecyl acrylate), and the resulting polymer was purified by precipitation, leading to a well-defined copolymer, $M_n \approx 10000$ and $D = 1.28$ (Figure S50). Interestingly, the DSC thermogram showed an observable T_m (≈ 40 °C) and T_g (at -16 °C), very similar temperatures to those of the discrete homopolymers (see Figure 9). This

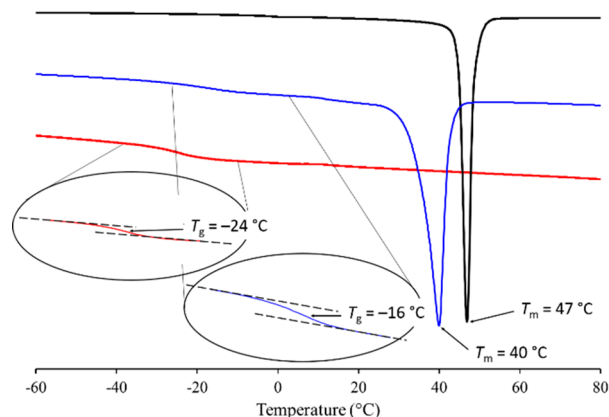


Figure 9. DSC thermograms collected for homopolymers of poly(cycloheptadecyl acrylate) (red) and poly(octadecyl acrylate) (black) as well as a diblock copolymer of these two monomers (blue).

suggests that microphase separation of the diblock copolymer is occurring in the bulk—despite the very similar chemical composition/hydrophobicity—likely promoted by the conformation and packing differences between the side chains. A diblock copolymer with blocks of ~ 25000 g/mol was targeted to improve separation; however, high dispersity indicated loss of end-group fidelity at high molecular weights.

To illustrate the tuning of thermal properties by modifying the architecture of the side-chain alkyl group, materials based on docosyl (C_{22}) acrylate were examined because they show promise in a variety of applications, but their high tendency to crystallize limits full utility.⁵⁵ To reduce this crystallinity, docosyl acrylate is often copolymerized with noncrystalline monomers, such as acrylic acid⁵⁶ or methyl methacrylate,⁵⁵ with significant incorporation of comonomer often required. For example, crystallinity was still observed in the copolymer of docosyl acrylate and acrylic acid at 86 mol % acrylic acid,⁵⁶ significantly decreasing the hydrophobicity and, in turn, functionality as an oil absorbant. We rationalized that copolymerization with macrocyclic hydrophobic monomers should significantly decrease the crystallinity of the polymer without reducing overall hydrophobicity. A series of random copolymers were therefore synthesized based on docosyl (L-22) acrylate and cyclohexadecyl (C-16) acrylate (specifically, 25, 40, 50, 60, 70, and 75 mol % cyclohexadecyl acrylate) with the observed phase transitions compared to the respective homopolymers (Figure 10). Significantly, the thermal transitions could be tuned from the highly crystalline poly(docosyl acrylate) homopolymer ($T_m = 67$ °C) to the amorphous poly(cyclohexadecyl acrylate) homopolymer ($T_g = -19$ °C), with the sharp melting transition being significantly decreased at only 40 mol % cyclohexadecyl acrylate and completely suppressed above 70 mol %. The enthalpy of fusion (ΔH_f) was

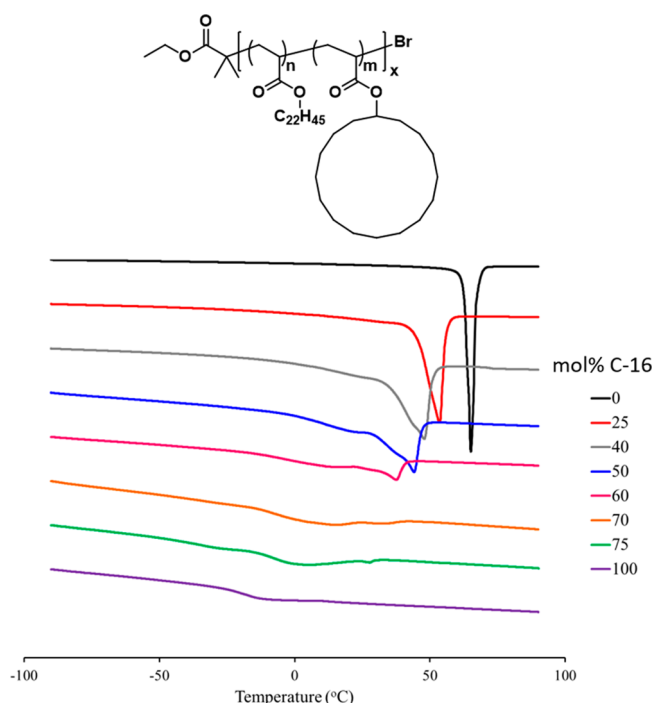


Figure 10. DSC thermograms collected for homopolymers of poly(cyclohexadecyl acrylate) (bottom), poly(docosyl acrylate) (top), and random copolymers of these two monomers in varying ratios. Legend indicates mol % cyclohexadecyl acrylate in the copolymer.

also significantly decreased from 110.1 J/g^{57,58} to 61.2, 44.7, and 37.7 J/g in the 25, 40, and 50 mol % poly(cyclohexadecyl acrylate) copolymers, indicating reduced crystallinity. Similar behavior was observed with random copolymers of octadecyl acrylate (C_{18}) and cyclododecyl acrylate (C_{12}) (Figure S51) with all copolymers showing high hydrophobicity and solubility in hexanes.

CONCLUSIONS

In conclusion, we describe the controlled radical polymerization of hydrophobic, macrocyclic side-chain monomers (C_{12} , C_{16} , and C_{17}) using photoinduced ATRP. These materials are obtained from readily available starting materials; in particular, cycloheptadecyl acrylate is prepared from civetone, found naturally in the musk oil of civet cats and used widely in the fragrance industry. Our selected method of photoinduced ATRP works equally well with both macrocyclic and linear hydrocarbon side chains, exhibiting good control over molar mass and dispersity. A high degree of chain-end fidelity also allows for the efficient in-situ generation of diblock copolymers. Significant differences in thermal properties were observed between these analogous acrylate building blocks with incorporation of the macrocyclic derivatives into random copolymers, minimizing the crystallinity of poly(docosyl acrylate) (C_{22}) and poly(octadecyl acrylate) (C_{18}) while maintaining the high hydrophobicity of the polymer. The synthetic advances reported in this study will allow new hydrophobic materials to be prepared with tunable properties based on the architecture of the side chains, leading to enhanced application as viscosity modifiers and oil absorbants.

■ ASSOCIATED CONTENT

● Supporting Information

The Supporting Information is available free of charge on the ACS Publications website at DOI: 10.1021/acs.macromol.8b01509.

NMR spectra, SEC chromatograms, MALDI spectra, and DSC thermograms (PDF)

■ AUTHOR INFORMATION

Corresponding Author

*(C.J.H.) E-mail: hawker@mrl.ucsb.edu.

ORCID

Nghia P. Truong: 0000-0001-9900-2644

Christopher M. Bates: 0000-0002-1598-794X

Craig J. Hawker: 0000-0001-9951-851X

Notes

The authors declare no competing financial interest.

■ ACKNOWLEDGMENTS

This work was supported by the National Science Foundation, Division of Materials Research under the Materials Research Science & Engineering Centers Program (DMR 1720256 (IRG-3)). The research reported here made use of shared facilities of the UCSB MRSEC (NSF DMR 1720256), a member of the Materials Research Facilities Network. S.B. and A.A. acknowledge the California NanoSystems Institute for an Elings Prize Fellowship in Experimental Science. A.A. is grateful to the European Union's Horizon 2020 research and innovation program for a Marie Curie Global Postdoctoral Fellowship, and S.B. is grateful to the National Science and Engineering Research Council of Canada for the Banting Postdoctoral Fellowship. N.P.T. acknowledges the award of a DECRA Fellowship from the Australian Research Council (DE180100076). We also sincerely thank Dr. Rachel Behrens for help with polymer characterization.

■ REFERENCES

- (1) Matyjaszewski, K.; Xia, J. Atom Transfer Radical Polymerization. *Chem. Rev.* **2001**, *101*, 2921–2990.
- (2) Matyjaszewski, K. Atom Transfer Radical Polymerization (ATRP): Current Status and Future Perspectives. *Macromolecules* **2012**, *45*, 4015–4039.
- (3) Moad, G.; Rizzardo, E.; Thang, S. H. Living Radical Polymerization by the RAFT Process. *Aust. J. Chem.* **2005**, *58*, 379–410.
- (4) Barner-Kowollik, C.; Davis, T. P.; Heuts, J. P. A.; Stenzel, M. H.; Vana, P.; Whittaker, M. RAFTing down under: Tales of missing radicals, fancy architectures, and mysterious holes. *J. Polym. Sci., Part A: Polym. Chem.* **2003**, *41*, 365–375.
- (5) Hawker, C. J.; Bosman, A. W.; Harth, E. New Polymer Synthesis by Nitroxide Mediated Living Radical Polymerizations. *Chem. Rev.* **2001**, *101*, 3661–3688.
- (6) Nicolas, J.; Guillaneuf, Y.; Lefay, C.; Bertin, D.; Gimes, D.; Charleux, B. Nitroxide-mediated polymerization. *Prog. Polym. Sci.* **2013**, *38*, 63–235.
- (7) Braunecker, W. A.; Matyjaszewski, K. Controlled/living radical polymerization: Features, developments, and perspectives. *Prog. Polym. Sci.* **2007**, *32*, 93–146.
- (8) Sauv e, E. R.; Tonge, C. M.; Paisley, N. R.; Cheng, S.; Hudson, Z. M. Cu(0)-RDRP of acrylates based on p-type organic semiconductors. *Polym. Chem.* **2018**, *9*, 1397–1403.
- (9) McKenzie, T. G.; Fu, Q.; Uchiyama, M.; Satoh, K.; Xu, J.; Boyer, C.; Kamigaito, M.; Qiao, G. G. Beyond Traditional RAFT: Alternative Activation of Thiocarbonylthio Compounds for Controlled Polymerization. *Adv. Sci.* **2016**, *3*, 1500394.
- (10) Trotta, J. T.; Fors, B. P. Organic Catalysts for Photocontrolled Polymerizations. *Synlett* **2016**, *27*, 702–713.
- (11) Boyer, C. A.; Miyake, G. M. Polymers and Light. *Macromol. Rapid Commun.* **2017**, *38*, 1700327.
- (12) Frick, E.; Anastasaki, A.; Haddleton, D. M.; Barner-Kowollik, C. Enlightening the Mechanism of Copper Mediated PhotoRDRP via High-Resolution Mass Spectrometry. *J. Am. Chem. Soc.* **2015**, *137*, 6889–6896.
- (13) Anastasaki, A.; Nikolaou, V.; Simula, A.; Godfrey, J.; Li, M.; Nurumbetov, G.; Wilson, P.; Haddleton, D. M. Expanding the Scope of the Photoinduced Living Radical Polymerization of Acrylates in the Presence of CuBr₂ and Me₆Tren. *Macromolecules* **2014**, *47*, 3852–3859.
- (14) Anastasaki, A.; Nikolaou, V.; Zhang, Q.; Burns, J.; Samanta, S. R.; Waldron, C.; Haddleton, A. J.; McHale, R.; Fox, D.; Percec, V.; Wilson, P.; Haddleton, D. M. Copper(II)/Tertiary Amine Synergy in Photoinduced Living Radical Polymerization: Accelerated Synthesis of ω -Functional and α,ω -Heterofunctional Poly(acrylates). *J. Am. Chem. Soc.* **2014**, *136*, 1141–1149.
- (15) Tasdelen, M. A.; Ciftci, M.; Yagci, Y. Visible Light-Induced Atom Transfer Radical Polymerization. *Macromol. Chem. Phys.* **2012**, *213*, 1391–1396.
- (16) Tasdelen, M. A.; Uygun, M.; Yagci, Y. Photoinduced Controlled Radical Polymerization in Methanol. *Macromol. Chem. Phys.* **2010**, *211*, 2271–2275.
- (17) Konkolewicz, D.; Schr oder, K.; Buback, J.; Bernhard, S.; Matyjaszewski, K. Visible Light and Sunlight Photoinduced ATRP with ppm of Cu Catalyst. *ACS Macro Lett.* **2012**, *1*, 1219–1223.
- (18) Wenn, B.; Martens, A. C.; Chuang, Y. M.; Gruber, J.; Junkers, T. Efficient multiblock star polymer synthesis from photo-induced copper-mediated polymerization with up to 21 arms. *Polym. Chem.* **2016**, *7*, 2720–2727.
- (19) Theriot, J. C.; Lim, C.-H.; Yang, H.; Ryan, M. D.; Musgrave, C. B.; Miyake, G. M. Organocatalyzed atom transfer radical polymerization driven by visible light. *Science* **2016**, *352*, 1082–1086.
- (20) Treat, N. J.; Sprafke, H.; Kramer, J. W.; Clark, P. G.; Barton, B. E.; Read de Alaniz, J.; Fors, B. P.; Hawker, C. J. Metal-Free Atom Transfer Radical Polymerization. *J. Am. Chem. Soc.* **2014**, *136*, 16096–16101.
- (21) Xu, J.; Jung, K.; Atme, A.; Shanmugam, S.; Boyer, C. A Robust and Versatile Photoinduced Living Polymerization of Conjugated and Unconjugated Monomers and Its Oxygen Tolerance. *J. Am. Chem. Soc.* **2014**, *136*, 5508–5519.
- (22) Xu, J.; Jung, K.; Boyer, C. Oxygen Tolerance Study of Photoinduced Electron Transfer–Reversible Addition–Fragmentation Chain Transfer (PET-RAFT) Polymerization Mediated by Ru(bpy)₃Cl₂. *Macromolecules* **2014**, *47*, 4217–4229.
- (23) Kottisch, V.; Michaudel, Q.; Fors, B. P. Photocontrolled Interconversion of Cationic and Radical Polymerizations. *J. Am. Chem. Soc.* **2017**, *139*, 10665–10668.
- (24) Rubens, M.; Latsrisaeng, P.; Junkers, T. Visible light-induced iniferter polymerization of methacrylates enhanced by continuous flow. *Polym. Chem.* **2017**, *8*, 6496–6505.
- (25) Allegranza, M. L.; DeMartini, Z. M.; Kloster, A. J.; Digby, Z. A.; Konkolewicz, D. Visible and sunlight driven RAFT photopolymerization accelerated by amines: kinetics and mechanism. *Polym. Chem.* **2016**, *7*, 6626–6636.
- (26) Shanmugam, S.; Xu, J.; Boyer, C. A logic gate for external regulation of photopolymerization. *Polym. Chem.* **2016**, *7*, 6437–6449.
- (27) Yeow, J.; Chapman, R.; Xu, J.; Boyer, C. Oxygen tolerant photopolymerization for ultralow volumes. *Polym. Chem.* **2017**, *8*, 5012–5022.
- (28) Anastasaki, A.; Oschmann, B.; Willenbacher, J.; Melker, A.; Van Son, M. H. C.; Truong, N. P.; Schulze, M. W.; Discekici, E. H.; McGrath, A. J.; Davis, T. P.; Bates, C. M.; Hawker, C. J. One-Pot Synthesis of ABCDE Multiblock Copolymers with Hydrophobic,

Hydrophilic, and Semi-Fluorinated Segments. *Angew. Chem., Int. Ed.* **2017**, *56*, 14483–14487.

(29) Shanmugam, S.; Xu, J.; Boyer, C. Photoinduced Electron Transfer–Reversible Addition–Fragmentation Chain Transfer (PET-RAFT) Polymerization of Vinyl Acetate and N-Vinylpyrrolidinone: Kinetic and Oxygen Tolerance Study. *Macromolecules* **2014**, *47*, 4930–4942.

(30) Boyer, C.; Atme, A.; Waldron, C.; Anastasaki, A.; Wilson, P.; Zetterlund, P. B.; Haddleton, D.; Whittaker, M. R. Copper(0)-mediated radical polymerisation in a self-generating biphasic system. *Polym. Chem.* **2013**, *4*, 106–112.

(31) Beers, K. L.; Matyjaszewski, K. The Atom Transfer Radical Polymerization of Lauryl Acrylate. *J. Macromol. Sci., Part A: Pure Appl. Chem.* **2001**, *38*, 731–739.

(32) Biedroń, T.; Kubisa, P. Atom-Transfer Radical Polymerization of Acrylates in an Ionic Liquid. *Macromol. Rapid Commun.* **2001**, *22*, 1237–1242.

(33) Boschmann, D.; Vana, P. Z-RAFT Star Polymerizations of Acrylates: Star Coupling via Intermolecular Chain Transfer to Polymer. *Macromolecules* **2007**, *40*, 2683–2693.

(34) Theis, A.; Feldermann, A.; Charton, N.; Davis, T. P.; Stenzel, M. H.; Barner-Kowollik, C. Living free radical polymerization (RAFT) of dodecyl acrylate: Chain length dependent termination, mid-chain radicals and monomer reaction order. *Polymer* **2005**, *46*, 6797–6809.

(35) Karaky, K.; Clisson, G.; Reiter, G.; Billon, L. Semicrystalline Macromolecular Design by Nitroxide-Mediated Polymerization. *Macromol. Chem. Phys.* **2008**, *209*, 715–722.

(36) Street, G.; Illsley, D.; Holder, S. J. Optimization of the synthesis of poly(octadecyl acrylate) by atom transfer radical polymerization and the preparation of all comblike amphiphilic diblock copolymers. *J. Polym. Sci., Part A: Polym. Chem.* **2005**, *43*, 1129–1143.

(37) Jang, J.; Kim, B. S. Studies of crosslinked styrene–alkyl acrylate copolymers for oil absorbency application. I. Synthesis and characterization. *J. Appl. Polym. Sci.* **2000**, *77*, 903–913.

(38) Çaykara, T.; Birlik, G. Swelling and Adsorption Properties of Hydrophobic Poly[(N-(3-(dimethylamino)propyl)methacrylamide)-co-(lauryl acrylate)] Hydrogels in Aqueous Solutions of Surfactants. *Macromol. Mater. Eng.* **2005**, *290*, 869–874.

(39) Schmidt, S. Acrylic block copolymer low temperature flow modifiers in lubricating oils. US Patent No. 20060185903, 2006.

(40) Harris, H. V.; Holder, S. J. Octadecyl acrylate based block and random copolymers prepared by ATRP as comb-like stabilizers for colloidal micro-particle one-step synthesis in organic solvents. *Polymer* **2006**, *47*, 5701–5706.

(41) Zhou, J.; Wang, L.; Dong, X.; Chen, T.; Yang, Q.; Tan, Q.; Wang, J. Study on synthesis of two-armed polymers containing a crown ether core and their self-assembly behaviors in selective solvents. *Eur. Polym. J.* **2007**, *43*, 2088–2095.

(42) Zhou, J.; Wang, L.; Dong, X.; Yang, Q.; Wang, J.; Yu, H.; Chen, X. Preparation of organic/inorganic hybrid nanomaterials using aggregates of poly(stearyl methacrylate)-b-poly(3-(trimethoxysilyl)propyl methacrylate) as precursor. *Eur. Polym. J.* **2007**, *43*, 1736–1743.

(43) Chatterjee, D. P.; Mandal, B. M. Triblock Thermoplastic Elastomers with Poly(lauryl methacrylate) as the Center Block and Poly(methyl methacrylate) or Poly(tert-butyl methacrylate) as End Blocks. Morphology and Thermomechanical Properties. *Macromolecules* **2006**, *39*, 9192–9200.

(44) Jakubowski, W.; Lutz, J. F.; Slomkowski, S.; Matyjaszewski, K. Block and random copolymers as surfactants for dispersion polymerization. I. Synthesis via atom transfer radical polymerization and ring-opening polymerization. *J. Polym. Sci., Part A: Polym. Chem.* **2005**, *43*, 1498–1510.

(45) Pitsikalis, M.; Siakali-Kioulafa, E.; Hadjichristidis, N. Block Copolymers of Styrene and Stearyl Methacrylate. Synthesis and Micellization Properties in Selective Solvents. *Macromolecules* **2000**, *33*, 5460–5469.

(46) Fleischhaker, F.; Haehnel, A. P.; Misske, A. M.; Blanchot, M.; Haremza, S.; Barner-Kowollik, C. Glass-Transition-, Melting-, and Decomposition Temperatures of Tailored Polyacrylates and Poly-methacrylates: General Trends and Structure–Property Relationships. *Macromol. Chem. Phys.* **2014**, *215*, 1192–1200.

(47) Daimon, H.; Kumanotani, J. Solvent effects on radical polymerization of cyclododecyl acrylate. I. Homopolymerization. *Makromol. Chem.* **1975**, *176*, 2359–2373.

(48) Samanta, S. R.; Anastasaki, A.; Waldron, C.; Haddleton, D. M.; Percec, V. SET-LRP of hydrophobic and hydrophilic acrylates in tetrafluoropropanol. *Polym. Chem.* **2013**, *4*, 5555–5562.

(49) Samanta, S. R.; Cai, R.; Percec, V. SET-LRP of semifluorinated acrylates and methacrylates. *Polym. Chem.* **2014**, *5*, 5479–5491.

(50) Samanta, S. R.; Sun, H.-J.; Anastasaki, A.; Haddleton, D. M.; Percec, V. Self-activation and activation of Cu(0) wire for SET-LRP mediated by fluorinated alcohols. *Polym. Chem.* **2014**, *5*, 89–95.

(51) Anastasaki, A.; Waldron, C.; Nikolaou, V.; Wilson, P.; McHale, R.; Smith, T.; Haddleton, D. M. Polymerization of long chain [meth]acrylates by Cu(0)-mediated and catalytic chain transfer polymerisation (CCTP): high fidelity end group incorporation and modification. *Polym. Chem.* **2013**, *4*, 4113–4119.

(52) Glass Transition Temperatures; <http://polymerdatabase.com/polymer%20physics/Polymer%20Tg.html>.

(53) Thermal Transitions of Homopolymers: Glass Transition & Melting Point; <https://www.sigmaaldrich.com/technical-documents/articles/materials-science/polymer-science/thermal-transitions-of-homopolymers.html>.

(54) Saikia, P. J.; Dass, N. N.; Baruah, S. D. Cocrystallization behavior of poly(n-docosyl acrylate) with n-docosanoic acid by X-ray and differential scanning calorimetry studies. *J. Appl. Polym. Sci.* **2005**, *97*, 2140–2146.

(55) Farag, R. K.; El-Saeed, S. M. Synthesis and characterization of oil sorbers based on docosanyl acrylate and methacrylates copolymers. *J. Appl. Polym. Sci.* **2008**, *109*, 3704–3713.

(56) Bisht, H. S.; Pande, P. P.; Chatterjee, A. K. Docosyl acrylate modified polyacrylic acid: synthesis and crystallinity. *Eur. Polym. J.* **2002**, *38*, 2355–2358.

(57) Jordan, E. F.; Feldeisen, D. W.; Wrigley, A. N. Side-chain crystallinity. I. Heats of fusion and melting transitions on selected homopolymers having long side chains. *J. Polym. Sci., Part A-1: Polym. Chem.* **1971**, *9*, 1835–1851.

(58) Mogri, Z.; Paul, D. R. Gas sorption and transport in poly(alkyl (meth)acrylate)s. I. Permeation properties. *Polymer* **2001**, *42*, 7765–7780.